

Effect of Electrode Length and AC Frequency on Mixing in a Diamond-Shaped Split-And-Recombine Electroosmotic Micromixer



Amrendra Kumar, Nirmal K. Manna, and Sandip Sarkar

Abstract Lab-on-a-chip (LOC) and microfluidic devices have gained more and more importance in biological and chemical fields. A homogeneous mix of multiple reagents and chemicals is often essential to assist the chemical and biological reactions. Electroosmotic flow is an attractive approach for enhancing the homogeneous mix of species in a micro-scale mixer. In this work, a two-dimensional microfluidic mixture with a diamond-shaped split-and-recombine structure, using commercial software package COMSOL Multiphysics is analyzed. The choice of suitable electrode length is made by performing a series of simulations. The influence of AC (alternating current) frequency on the mixing of two fluids is also studied. The mixing efficiency of the micromixer initially increases with an increase in AC frequency and after reaching a maximum value, it starts decreasing. The best suited AC potential frequency for different electrode lengths is different. It is found from the results that the increase in electrode length does not always increase the mixing efficiency of the micromixer. The electrode length of such mixers critically affects the mixing efficiency and the suitable electrode length results in improved mixing of fluids.

Keywords Micromixer · Electroosmosis · Mixing efficiency · Electrode length

1 Introduction

With the advances in lab-on-a-chip (LOC) and microfluidic devices, microfluidics has gained more and more importance in biological and chemical fields. Mixing and pumping of several reagents and chemicals are often crucial and necessary to assist

A. Kumar · N. K. Manna · S. Sarkar (✉)

Department of Mechanical Engineering, Jadavpur University, Kolkata 700032, India

e-mail: thesandipsarkar3@gmail.com; sandipsarkar.mech@jadavpuruniversity.in

A. Kumar

e-mail: amrendraju@gmail.com

N. K. Manna

e-mail: nirmalkmannaju@gmail.com

© The Author(s), under exclusive license to Springer Nature Singapore Pte Ltd. 2023

T. S. Sudarshan et al. (eds.), *Recent Advancements in Mechanical Engineering*,

Lecture Notes in Mechanical Engineering,

https://doi.org/10.1007/978-981-19-3266-3_7

chemical and biological reactions [1, 2]. Usually, the turbulent mixing of fluids is not possible, due to the small dimensions of the microfluidic devices [3]. Mixing of liquids in a micro-scale takes place primarily due to diffusional mixing. The mixing efficiency of such small-scale devices is not up to the mark as per production and testing levels.

The method of engendering vortices in micro-scale channels has been reported by many scholars and generally, it is divided into two groups, namely active group and passive group [4, 5]. The passive group mainly incorporates special geometries [6, 7] of microchannels and various types of obstacle shapes [8–11] or grooves [12–14] accommodated in micro-scale channels to generate vortices in the laminar flow field. This group of micromixers does not require any external source of energy, but these channels are heavily dependent on complex designs with special structures, thus increasing the fabrication difficulty. By contrast, external energy such as magnetic energy [4, 15], acoustic energy [16], and electrical energy [17, 18] is applied in an active group of micromixers to generate vortices.

The electrically actuated active (electroosmotic) method is an attractive approach for enhancing mixing. Electroosmotic mixers have a simple design, convenient working procedures, and enhanced efficiency. By applying low potential alternating currents (AC) using microelectrodes along the channel walls, the laminar flow field can be distorted and a chaotic state of the flow field is generated in the microchannel mixer. This enhances the number of interactions at the molecular level by stretching and squeezing the fluid flow, thereby increasing the mixing efficiency. These advantages have made electroosmotic technology popular among scientists and engineers studying microfluidic technology and analysis system. Huang et al. [19] developed an innovative electroosmotic micromixer with various electrode arrangements on the base surface of the Y-mixing channel, which employed micro-vortex patterns to enhance the mixing in a lab-on-a-chip device. Zhang et al. [20] numerically studied the controlling the fluid flow rate in the micro-mixer by using induced electro-osmosis in the mixer channel to generate a flow field with vortices in the fluid solution, and designed an electrokinetic microchannel mixer network that can increase the microchannel mixing efficiency with significantly small mixing length. Zhao et al. [21] studied the flow behavior of power-law fluid in a slit microchannel under the influence of the electroosmotic flow phenomenon. Nayak et al. [22] implemented the model of sequencing heterogeneous potentials on the micro-channel surface and concluded that the mixing of a Newtonian fluid in micro-channels can be improved by the pressure gradient and vortices generated by the electric field. Sasaki et al. [23] designed an AC electroosmotic Y-microchannel mixer. The bottom surface of the mixer is having a coplanar pair of sinusoidal electrodes. AC electric potential is applied to the sinusoidal electrodes and AC frequency (1–5 kHz) is varied to study its effects on mixer performance. The maximum mixer mixing efficiency of nearly 92% is reported at 20 V potential and 1 kHz frequency.

In this paper, based on mixing efficiency, a primary parameter of micro-channel mixers, the effect of electrode length for the microfluidic mixture with a diamond split-and-combine structure is analyzed. Furthermore, the influence of AC (alternating current) frequency on the mixing of fluids is also studied.

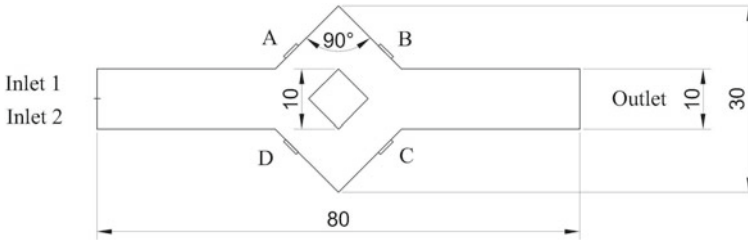


Fig. 1 Schematic of the rhombus-shaped annular micromixer

2 Numerical Model

2.1 Microfluidic Problem Model and Formulation

The schematic of the rhombus-shaped annular active micromixer is presented in Fig. 1. The channel depth to width ratio is considered sufficiently large to justify the 2D geometry assumption for the microfluidic mixer. Two fluids enter into the straight inlet channel through inlet 1 and 2, respectively. The width of the inlets (1 and 2 both) is $5 \mu\text{m}$, resulting in a combined width of the main channel as $10 \mu\text{m}$, the total length of the main channel is $80 \mu\text{m}$. The two liquids initially pass through this main channel and then enter the rhombus-shaped annular micro-mixing chamber with an outer rhombus diagonal of $d_0 = 30 \mu\text{m}$ and inner rhombus diagonal of $d_i = 10 \mu\text{m}$. Four microelectrodes (namely A, B, C, and D) are mounted on the wall of the outer rhombus of the annular mixing chamber with an angular displacement of 45° with axial direction and thus making an angle of 90° with each other. The electrode length is varied from 2 to $7 \mu\text{m}$. The initial concentration (c_0) of the liquid entering inlets 1 and 2 is considered as 1 mol/m^3 and 0 mol/m^3 , respectively. A constant value of the zeta potential is assumed on the mixer wall. The micro-electrodes are actuated with time-varying sinusoidal AC with alternating polarity, but the same potential amplitude and AC frequency. This leads to vortices generation within the annular chamber, leading to the mixed liquid flowing out of the main channel outlet.

2.2 Governing Equations and Scheme

The liquid solution is assumed as a viscous-incompressible, Newtonian and the flow is considered as laminar. Thus, the flow field is governed by the following equations of continuity and momentum:

$$\nabla \cdot \mathbf{u} = 0 \quad (1)$$

$$\rho \cdot \left(\frac{\partial u}{\partial t} + (u \cdot \nabla)u \right) = -\nabla p + \mu \nabla^2 u \quad (2)$$

The convection–diffusion equation is implemented to describe the concentration distribution of solute in fluids:

$$\frac{\partial c}{\partial t} + \nabla \cdot (-D \nabla c) = -u \cdot \nabla c \quad (3)$$

In the above equations, u represents the velocity vector (0.1 mm/s at the inlet), ρ (1000 kg/m³) is the fluid density, p is the pressure (Pa), t refers to the time (s) and μ is the dynamic viscosity coefficient of the fluid (10³ Pa s), $\mu \nabla^2 u$ is the viscous force experienced by the fluid, D (0.6 × 10⁻¹¹ m²/s) is the diffusion coefficient. It may be noted that the properties of the fluid are assumed to be similar to that of the liquid water.

The Helmholtz–Smoluchowski (HS) relation between the slip velocity and the applied AC field is chosen over the thin EDL (electric double layer) force. Thus, at the microchannel wall, an electroosmotic slip velocity condition is applied instead of the thin EDL with the HS relation as follows:

$$u = \frac{\varepsilon_0 \varepsilon_r \xi_0}{\eta} \nabla_t V \quad \text{Here, } \nabla_t V = E_t = E - (n \cdot E)n \quad (4)$$

where, $\varepsilon_0 = 8.854 \times 10^{-12}$ C/Vm is the permittivity of vacuum, $\varepsilon_r = 80.2$ is the relative permittivity of the water, ξ_0 is the zeta potential (−0.1 V), V is the applied potential (0.1 V), E refers to the bulk electrical field.

The current balance within the mixer is as follows:

$$\nabla \cdot (\sigma \nabla V) = 0 \quad (5)$$

where σ is the fluid solution conductivity and $\sigma \nabla V$ is the current density. The electric insulation condition is considered on all the boundaries except electrodes.

At the electrodes AC potential is imposed as follows:

$$V = \pm V_0 \sin(\omega t) \quad \text{Here, } \omega = 2\pi f \quad (6)$$

where V_0 is the applied voltage amplitude, ω is the angular frequency, and f represents the AC frequency.

The performance analysis parameter, mixing efficiency ($\eta\%$) is introduced to analyze the fluid mixing is as follows:

$$\eta(\%) = \left(1 - \frac{\int_{y_1}^{y_2} |c - c_\infty| dy}{\int_{y_1}^{y_2} |c_0 - c_\infty| dy} \right) \times 100\% \quad (7)$$

Table 1 Grid independence study at $t = 0.5$ s for $u = 0.1$ mm/s, $V_0 = 0.1$ V, $L_e = 5$ μ m and $f = 12$ Hz

Sr. No	Mesh	Number of elements	Mixing efficiency (%)
1	G1	3059	84.96
2	G2	3739	81.60
3	G3	4358	80.15
4	G4	7488	79.22
5	G5	8559	79.31

where c_0 represents the totally unmixed solution concentration and c_∞ represents the totally mixed solution concentration. Also, y_1 represents the upper sectional limit and y_2 represents the lower sectional limit at a particular cross section of the microchannel. The magnitude of η varies from 0 to 100%, representing the mixing performance of the micromixer.

2.3 Grid Independence Study and Model Validation

In the present study, FEM (finite element method) package COMSOL Multiphysics is used for solving all of the mathematical equations. First, a two-dimensional structure is built and the physical properties and appropriate boundary conditions are set. Then, four different mesh sizes with unstructured triangular shapes, namely G1, G2, G3, G4, and G5 consisting of 3059, 3739, 4358, 7488, and 8559 number of elements, respectively, are chosen to discover the optimum mesh element size. The mixing efficiency percentage at $t = 0.5$ s for $u = 0.1$ mm/s, $V_0 = 0.1$ V, $L_e = 5$ μ m and $f = 12$ Hz at the outlet of the micromixer for all the grid sizes is shown in Table 1. As the deviation of the mixing efficiency between G4 and G5 is negligible, thus G4 mesh size with 7458 elements is considered for further simulation.

To verify the accuracy of the present numerical scheme, the results obtained with the electrokinetic micromixer demonstrated by Wu and Li [17] are simulated. Normalized concentration at different heights of cross section (at $x = 500$ μ m) is obtained from the experimental work of Wu and Li [17] and current numerical scheme is shown in Table 2. The good agreement of results obtained from the current numerical scheme with the reported work ascertains the accuracy of the numerical model.

3 Results and Discussion

In the absence of AC electrical potential in the micromixer, the laminar flow field leads to only molecular diffusional mixing. This can be observed in Fig. 2. By applying AC potential, vortices are generated and the laminar flow field is distorted.

Table 2 Model Validation with experimental results of Wu and Li for $E = 50$ V/cm at $x = 500 \mu\text{m}$ downstream from the hurdles

Sr. No	Cross-sectional height (y in μm)	Normalized concentration	
		Experimental result of Wu and Li [17]	Numerical result of present study
1	50.103	0.4162	0.4341
2	101.733	0.4753	0.4764
3	147.217	0.4993	0.5067
4	201.068	0.5502	0.5468
5	250.148	0.5931	0.5849

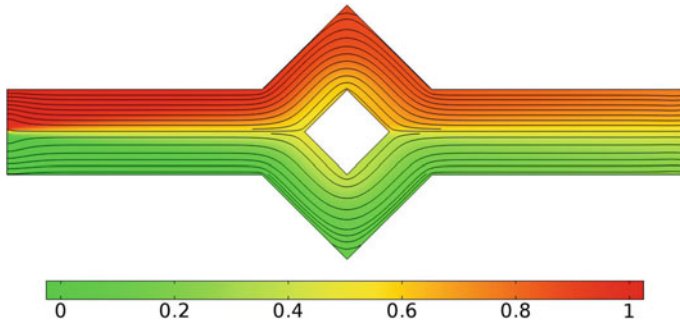


Fig. 2 Concentration and streamline plot without AC electric potential

This increases the number of interactions by stretching and overlapping of fluids at the molecular level and mixing is increased (Fig. 3).

Figure 4 shows the continuous change in mixing efficiency throughout the simulation time for electrode length $L_e = 5 \mu\text{m}$, keeping the other parameters fixed apart from frequency. The frequency is varied from 2 to 24 Hz. It can be observed from the

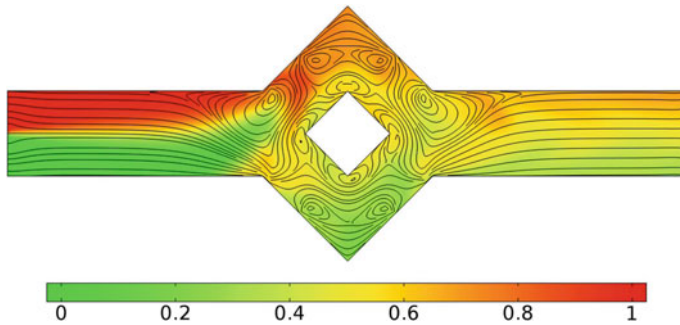


Fig. 3 Concentration and streamline plot with AC electric potential

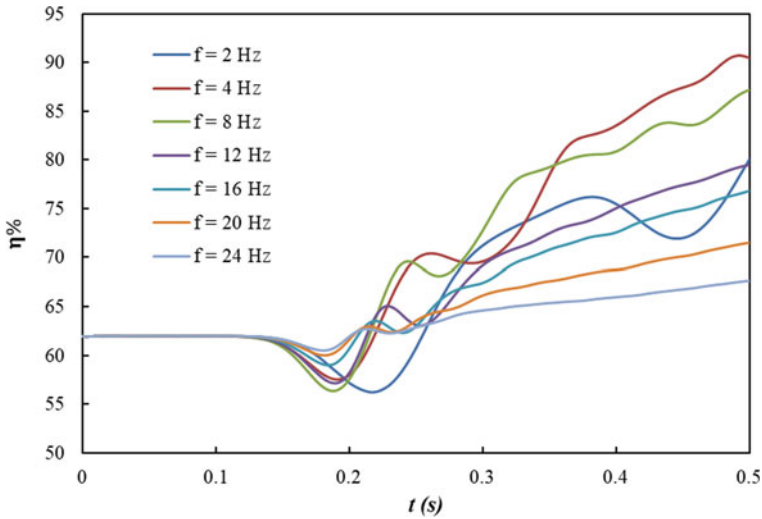


Fig. 4 Mixing efficiency variation with time for electrode length $L_c = 5 \mu\text{m}$ for $f = 2$ to 24 Hz

figure that with a change in the frequency the mixing efficiency changes dramatically. And for a particular frequency of 4 Hz, the maximum efficiency of approximately 90% at the end of simulation time is obtained.

In order to affirm that if this frequency of 4 Hz is the best frequency of operation, another electrode length of $7 \mu\text{m}$ is studied keeping the other parameters constant. Figure 5 shows the continuous change in mixing efficiency throughout the simula-

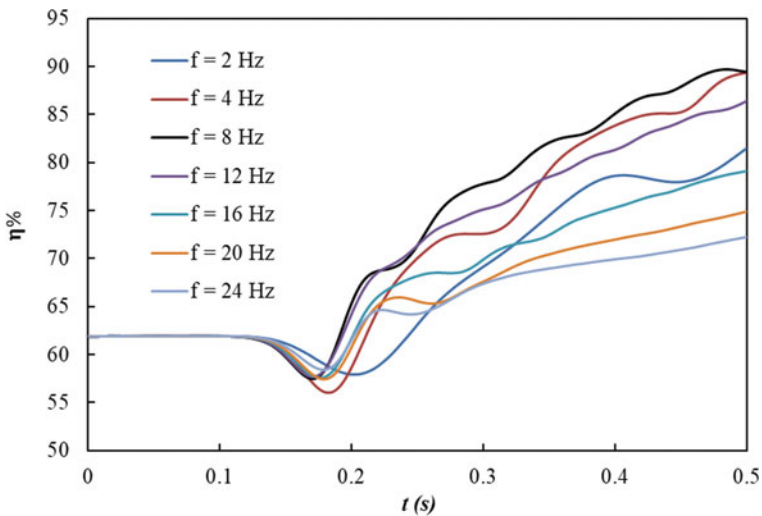


Fig. 5 Mixing efficiency variation with time for electrode length $L_c = 7 \mu\text{m}$ for $f = 2$ to 24 Hz

tion time for electrode length $L_e = 7 \mu\text{m}$. It can be observed from the figure that the frequency of 8 Hz is the best suited for the operation of the micromixer with an electrode length of $L_e = 7 \mu\text{m}$. These observations suggest that the change in electrode length of the micromixer affects the mixing efficiency, the best-suited frequency for the operation, and detailed analysis of the electrode length is needed.

In order to understand the relation between the electrode length and frequency the detailed analysis is done and electrode length is varied from $L_e = 2$ to $7 \mu\text{m}$ for frequency variation of $f = 2$ to 24 Hz . Figures 6 and 7 together show the effect of electrode length change and frequency change on mixing efficiency at time $t = 0.5 \text{ s}$. From Fig. 6, it can be observed that there is no specific trend observed for a specific frequency of operation on change in electrode length. At the two largest values of frequencies of 20 and 24 Hz, an approximately linear increase in mixing efficiency can be observed with an increase in electrode length. Though the linear trend is not observed for the frequencies of 8, 12, 16 Hz but the maximum efficiency is observed at the maximum electrode length of $L_e = 7 \mu\text{m}$. For $f = 2 \text{ Hz}$ the maximum efficiency is observed at electrode length of $L_e = 6 \mu\text{m}$, whereas for 4 Hz frequency of operation the maximum mixing efficiency of 92.82% is observed at an electrode length of $L_e = 4 \mu\text{m}$. Figure 6 indicates that initially with an increase in frequency the mixing efficiency increases for all the electrode lengths and then starts decreasing with a further increase in the frequency. Also, it is found that the best suited AC frequency in the cogent range of study is $f = 4 \text{ Hz}$.

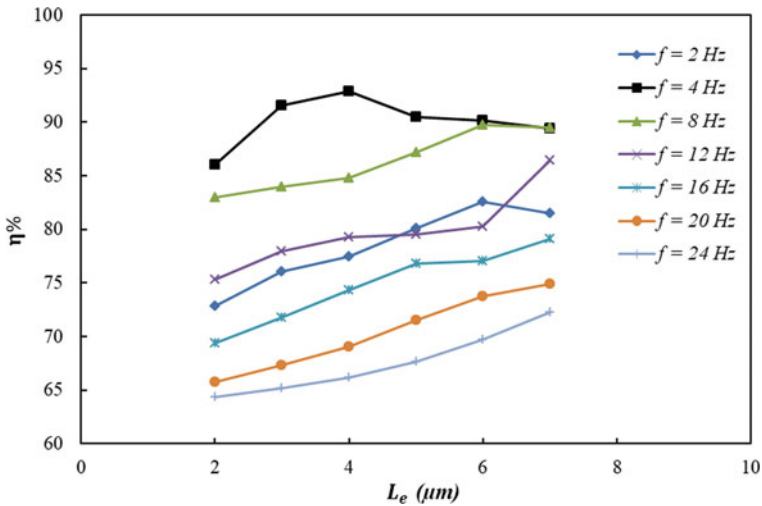


Fig. 6 Mixing efficiency variation with electrode length for $f = 2$ to 24 Hz at time $t = 0.5 \text{ s}$

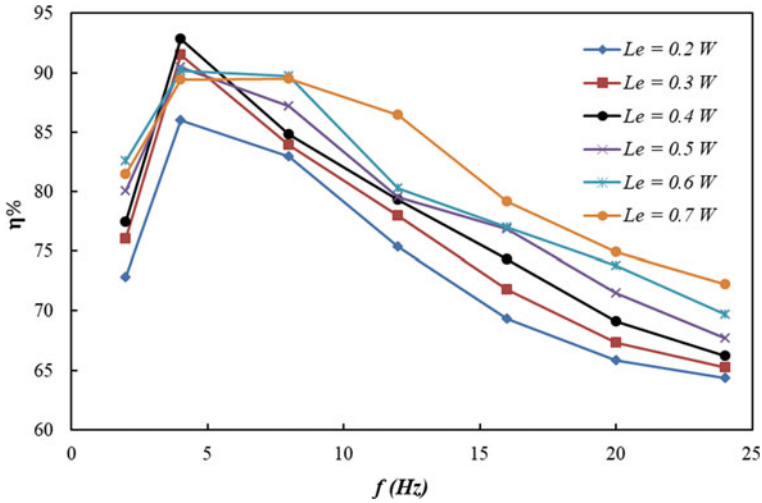


Fig. 7 Mixing efficiency variation with frequency for $L_e = 2$ to $7 \mu\text{m}$ at time $t = 0.5 \text{ s}$

4 Conclusion

In the present work, a two-dimensional rhombus-shaped annular AC micromixer equipped with four micro-electrodes is investigated numerically. A detailed analysis of the influence of electrode length and AC electrical frequency on the mixing characteristics of the microfluidic mixture is performed. Based on the studied model and suitable assumptions, the important outcomes can be summarized as follows:

- The application of AC potential distorts the flow field and the mixing efficiency of the electroosmotic mixer is greatly enhanced.
- The electrode length of the electroosmotic mixer critically affects the mixing efficiency. An increase in electrode length may increase or decrease the mixing efficiency of the micromixer. At high frequency, an increase in electrode length increases the mixing efficiency.
- The mixing efficiency of the micromixer initially increases with an increase in frequency and after reaching a maximum value, it starts decreasing.
- The best suited AC potential frequency for different electrode lengths is different. And the premier mixing efficiency is observed for the electrode length $L_e = 4 \mu\text{m}$ and frequency $f = 4 \text{ Hz}$.

References

1. Kim BJ, Yoon SY, Lee KH, Sung HJ (2009) Development of a microfluidic device for simultaneous mixing and pumping. *Exp Fluids* 46:85–95

2. Chakraborty S, Ray S (2008) Mass flow-rate control through time-periodic electro-osmotic flows in circular microchannels. *Phys Fluids* 20:083602
3. Heo HS, Suh YK (2005) Enhancement of stirring in a straight channel at low reynolds-numbers with various block-arrangement. *J Mech Sci Technol* 19:199–208
4. Chen Y, Kim CN (2018) Numerical analysis of the mixing of two electrolyte solutions in an electromagnetic rectangular micromixer. *J Ind Eng Chem* 60:377–389
5. Mondal B, Mehta SK, Patowari PK, Pati S (2019) Numerical study of mixing in wavy micromixers: comparison between raccoon and serpentine mixer. *Chem Eng Process* 136:44–61
6. Li J, Xia G, Li Y (2013) Numerical and experimental analyses of planar asymmetric split-and-recombine micromixer with dislocation sub-channels. *J Chem Technol Biotechnol* 88:1757–1765
7. Zhou T, Xu Y, Liu Z, Joo SW (2015) An enhanced one-layer passive microfluidic mixer with an optimized lateral structure with the dean effect. *J Fluids Eng* 137(9):091102
8. Miranda JM, Oliveira H, Teixeira JA, Vicente AA, Correia JH, Minas G (2010) Numerical study of micromixing combining alternate flow and obstacles. *Int Commun Heat Mass Transfer* 37(6):581–586
9. Cheri MS, Latifi H, Moghaddam MS, Shahraki H (2013) Simulation and experimental investigation of planar micromixers with short-mixing-length. *Chem Eng J* 234:247–255
10. Mondal B, Pati S, Patowari PK (2019) Analysis of mixing performances in microchannel with obstacles of different aspect ratios. *Proc Inst Mech Eng Part E: J Process Mech Eng* 233(5):1045–1051
11. Borgohain P, Arumughan J, Dalal A, Natarajan G (2018) Design and performance of a three-dimensional micromixer with curved ribs. *Chem Eng Res Des* 136:761–775
12. Hossain S, Husain A, Kim KY (2011) Optimization of micromixer with staggered herringbone grooves on top and bottom walls. *Eng Appl Comput Fluid Mech* 5(4):506–516
13. Jung SY, Park JE, Kang TG, Ahn KH (2019) Design optimization for a microfluidic crossflow filtration system incorporating a micromixer. *Micromachines* 10(12):836
14. Yoshimura M, Shimoyama K, Misaka T, Obayashi S (2019) Optimization of passive grooved micromixers based on genetic algorithm and graph theory. *Microfluid Nanofluid* 23(30):30
15. Dallakehnejad M, Mirbozorgi SA, Niazmand H (2019) A numerical investigation of magnetic mixing in electroosmotic flows. *J Electrostat* 100:103354
16. Rasoulia MR, Tabrizian M (2019) An ultra-rapid acoustic micromixer for synthesis of organic nanoparticles. *Lab on a Chip* 19(19):3316–3325
17. Wu Z, Li D (2008) Micromixing using induced-charge electrokinetic flow. *Electrochim Acta* 53:5827–5835
18. Seo HS, Han B, Kim YJ (2012) Numerical study on the mixing performance of a ring-type electroosmotic micromixer with different obstacle configurations. *J Nanosci Nanotechnol* 12:4523–4530
19. Huang SH, Wang SK, Khoo HS, Tseng FG (2007) AC electroosmotic generated in-plane microvortices for stationary or continuous fluid mixing. *Sens Actuators, B Chem* 125:326–336
20. Zhang F, Daghighi Y, Li D (2011) Control of flow rate and concentration in microchannel branches by induced charge electrokinetic flow. *J Colloid Interface Sci* 364:588–593
21. Zhao C, Zholkovskij E, Masliyah JH, Yang C (2008) Analysis of electroosmotic flow of power-law fluids in a slit microchannel. *J Colloid Interface Sci* 326:503–510
22. Nayak AK (2014) Analysis of mixing for electroosmotic flow in micro/nano channels with heterogeneous surface potential. *Int J Heat Mass Transf* 75:135–144
23. Sasaki N, Kitamori T, Kim HB (2010) Experimental and theoretical characterization of an AC electroosmotic micromixer. *Anal Sci* 26:815–819